

Peaked Density Profiles in Circular-Limiter H Modes on the TFTR Tokamak

C. E. Bush,^(a) R. J. Goldston, S. D. Scott, E. D. Fredrickson, K. McGuire, J. Schivell, G. Taylor, Cris W. Barnes,^(b) M. G. Bell, R. L. Boivin, N. Bretz, R. V. Budny, A. Cavallo, P. C. Efthimion, B. Grek, R. Hawryluk, K. Hill, R. A. Hulse, A. Janos, D. W. Johnson, S. Kilpatrick, D. M. Manos, D. K. Mansfield, D. M. Meade, H. Park, A. T. Ramsey, B. Stratton, E. J. Synakowski, H. H. Towner, R. M. Wieland, M. C. Zarnstorff, and S. Zweben

Princeton Plasma Physics Laboratory, Princeton University, Princeton, New Jersey 08543

(Received 2 April 1990)

Circular-limiter H modes are obtained on the TFTR tokamak during high-power neutral-beam heating. The transition is usually from the supershot to the H mode rather than the usual L to H transition, and thus is obtained in a low-recycling environment with core fueling mainly from the heating beams. As a result, the density and pressure profiles are highly peaked at the center. The global confinement time τ_E is enhanced over L -mode scaling by up to ≈ 2.5 times. The onset of edge-localized MHD modes shortly after the H -mode transition appears to limit τ_E . Limiter H modes of up to 1.5 s duration have been realized.

PACS numbers: 52.55.Pi, 52.25.Gj, 52.50.Gj, 52.55.Fa

Limiter H -mode plasmas were first reported on JFT-2M.¹⁻³ Since that initial report, limiter H -mode studies have been carried out on other tokamaks.^{4,5} The appeal of circular-limiter H -mode plasmas lies in the possibility of obtaining good confinement without a divertor or shaping coils to obtain elongated plasmas. This is the first report of H -mode plasmas with highly centrally peaked density profiles and of significantly enhanced confinement in circular-limiter H modes. This regime may be attractive for future α -heated tokamaks such as the Compact Ignition Tokamak (CIT) and the International Thermonuclear Experimental Reactor (ITER), since numerical studies show that the global energy confinement time τ_E required for ignition decreases as the n_e and T_e profiles become more peaked. Thus, TFTR offers the possibility of studying and comparing the physics of the supershot,⁶ H -mode, and L -mode⁷ regimes on the same tokamak.

The main sign of the divertor H mode, first reported for neutral-beam-injection- (NBI-) heated discharges in ASDEX,⁸ was a sudden transition (often within 2 ms or less) from the "low confinement" or L mode to the "high confinement" or H mode. The improved confinement was attributed in part to the establishment of a transport barrier at the plasma edge which reduced the particle and energy transport. D_α light at the periphery decreased sharply; the electron temperature profile developed an edge pedestal; the electron density profile became broad and flat with a steep edge gradient; and τ_E could improve by a factor of 2 or more over L -mode values. Edge-localized MHD modes⁹ (ELMs) were often triggered, causing periodic spoiling of the enhanced confinement and rapid expulsion of particles, energy, and impurities from the edge plasma. Most of these characteristics were also observed in the JFT-2M limiter H modes,^{1,2} although smaller improvements in confinement could occur.³ The main results for TFTR H modes re-

ported here are (a) the density profiles are unique for H modes in that they can be highly peaked at the center; (b) the characteristic H -mode signatures, a drop in D_α light and increases in n_e and T_e profiles at the plasma edge, are usually observed; (c) the global energy confinement time τ_E can be > 2.5 times the L -mode value; (d) the ELM instability is observed for nearly all TFTR H modes; and (e) the parameter range in which these H modes are obtained is relatively broad.

H modes have been obtained on TFTR for plasma current $I_p = 0.8$ – 1.7 MA, toroidal field $B_\phi = 3.0$ – 5.2 T, major radius $R_p = 2.45$ – 2.60 m, minor radius $a_p = 0.79$ – 0.95 m, cylindrical safety factor $q_c = 3.5$ – 6.8 ($q_\psi = 4.3$ – 10.4 , with most > 6.0), and NBI powers P_b of 11–28 MW. Generally, the higher P_b values were required to obtain H modes at the higher values of I_p . All TFTR H -mode shots were initially deuterium target plasmas subsequently heated with deuterium NBI except for three helium target plasmas. Circular-limiter H -mode plasmas were obtained on TFTR only during NBI heating. Beam heating pulses of 0.5–2.0 s were used. Bi-directional beam heating apparently is a requirement, with slightly counter-dominated injection being favorable. A unique feature of TFTR H -mode plasmas is that they are results of transitions from the supershot to the H regime rather than the usual L -mode to H -mode transition. In order to obtain supershots, the graphite limiter on TFTR must be highly conditioned, i.e., degassed,¹⁰ thus resulting in low-recycling limiters. The combination of high-power NBI and low-recycling limiters results in central beam fueling, and consequently in transitions to limiter H -mode plasmas which are highly peaked at the center. The range in \bar{n}_e was 2.2×10^{19} to $4.5 \times 10^{19}/\text{m}^3$ for H -mode plasmas obtained under low-recycling conditions. In all cases the effective limiter was a toroidally symmetric inner belt of carbon tile extending $\pm 60^\circ$ poloidally from the midplane.

The longest duration of an *H*-mode plasma realized in TFTR is 1.5 s, apparently limited only by the 2-s beam pulse used. Time evolutions of various parameters for this plasma are shown in Fig. 1, and most of the usual phenomena associated with the *H* mode are evident. The transition on TFTR is often, but not always, signaled by a decrease in the D_α signal. Transitions to the *H* mode with little or no drop in main-chamber D_α have also been reported for other tokamaks.¹¹ Time delays (after the beams turn on) before the transition to the *H* mode in TFTR can be 150 to > 600 ms. For the discharge of Fig. 1, NBI begins at 4.0 s and the transition takes place after 390 ms of heating. The time it takes for the D_α and C II intensities to fall is ≈ 50 ms, compared to < 2 ms for transitions in divertor *H* modes. Increases in edge ($r/a > 0.8$) n_e , T_e , and T_i are clear in Figs. 1(c)–1(e). The edge T_i (at $r/a = 0.9$) as measured by charge-exchange recombination spectroscopy (CHERS) increases from ≈ 1 to ≈ 2 keV at the transition, while the edge toroidal velocity (also from CHERS), $v_\phi(r/a = 0.9)$, decreases by a factor of 2.

The increase in electron stored energy E_e obtained for this shot [Fig. 1(h)] is typical for the limiter *H* modes observed in TFTR. However, the total stored energy E_{tot} either remains constant or decreases slightly. In the plasma illustrated in Fig. 1, E_{tot} remained relatively constant during the transition, and then decreased at the onset of ELMs. The decrease in E_{tot} is reflected in the decrease, beginning at about 4.5 s, in the global

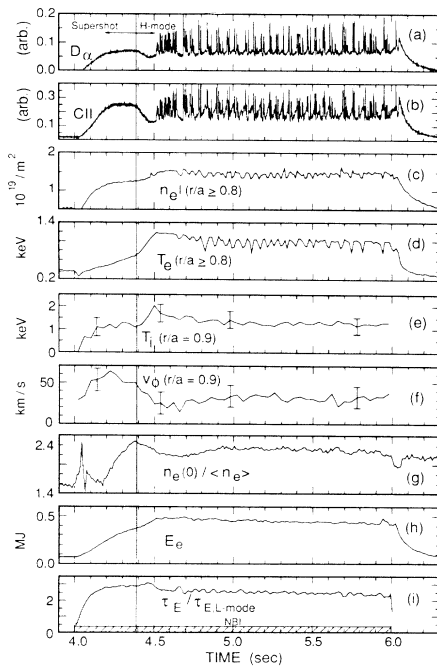


FIG. 1. Characteristics of a TFTR limiter *H* mode of 1.5 s duration. The time variation of D_α , C II, edge $n_e l$ and T_e , T_i , v_ϕ , density peaking factor [$n_e(0)/\langle n_e \rangle$], E_e , and $\tau_E/\tau_{E,L\text{-mode}}$ are plotted. $R = 2.45$ m, $a = 0.8$ m, $B_0 = 4$ T, $I_p = 0.8$ MA, $P_b = 11$ MW (balanced), and $\bar{n}_e = 2.5 \times 10^{13}/\text{cm}^3$. Shot No. 42935.

confinement [see Fig. 1(i)] from its value during the initial supershot phase. However, for the remainder of the discharge, ≈ 13 energy confinement times, τ_E remains near 110 ms or > 2.3 times the *L*-mode value. This is evident from Fig. 1(i) which is a plot of the ratio of τ_E to $\tau_{E,L\text{-mode}}$, where the latter is given by⁷

$$\tau_{E,L\text{-mode}} = 0.037 \frac{I_p}{1 \text{ MA}} \left(\frac{P_b}{1 \text{ MW}} \right)^{-0.5} \times \left(\frac{R_p}{1 \text{ m}} \right)^{1.75} \left(\frac{a_p}{1 \text{ m}} \right)^{-0.37}$$

Profiles of electron temperature and density and ion temperature, $T_e(R)$, $n_e(R)$, and $T_i(R)$, respectively, are plotted in Figs. 2(a)–2(c) at several times of the discharge of Fig. 1. Profiles at times during the supershot phase (4.3 and 4.4 s), at the end of the transition (4.5 s), and 50 ms after the initial ELM burst (at 4.55 s) are included. The profile shape at 4.55 s is typical for the remainder of the beam pulse. The $n_e(R)$ profiles of Fig. 2(a) are clearly highly peaked and in contrast to the flat density profiles obtained for the *H* mode on other tokamaks. During the transition, the largest fractional increase in $n_e(R)$ is for the edge plasma at $R \leq 180$ cm (inner edge), and at 320 cm (outer edge). This may be seen by comparing the $n_e(R)$ profile at 4.4 s to that at 4.5 s. In contrast, during the time evolution of the supershot phase (up to 4.4 s), the core density increases rapidly while there is little or no change in the edge density (compare the profiles for 4.3 and 4.4 s). For su-

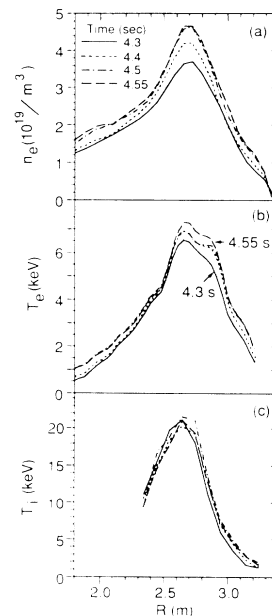


FIG. 2. Profiles of $n_e(R)$, $T_e(R)$, and $T_i(R)$ for the discharge of Fig. 1. Data for four times are included, during the supershot phase (4.3 and 4.4 s), at the end of the transition (4.5 s), and 50 ms after (at 4.55 s) the first ELM. $F_{ne} \approx 2.2$ at 4.55 s.

pershots which do not result in transitions to the *H* mode, $n_e(\text{center})$ continues to increase and the peaking factor, $F_{ne} = n_{e0}/\langle n_e \rangle$, can be > 3.0 . For the discharge of Figs. 1 and 2, F_{ne} has a maximum value of 2.5 during the supershot phase and is only slightly lower (due to the increase in n_e at the edge), ≈ 2.3 , for the duration of the *H*-mode phase. The corresponding pressure-profile peaking factor for the *H*-mode phase is $p_{e0}/\langle p_e \rangle = 5.0$. The ion temperature profile is also highly peaked with $T_i(\text{center}) > 20 \text{ keV} \approx 3T_e(\text{center})$.

Plasma fluctuations have been studied¹² at the transition and during the *H*-mode phase of TFTR limiter *H* modes. During the transition, the magnetic fluctuations in the range 15–25 kHz increase, while the high-frequency magnetic fluctuations in the range 150–200 kHz decrease. The improving confinement of the edge plasma appears to be stopped by ELM activity, which begins just after $t = 4.5 \text{ s}$ for the discharge of Fig. 1. The ELM instability is detected as intense bursts of D_α and C II light using arrays of detectors which view along chords perpendicular to the plasma column. In contrast to “*q* mode”¹³ but in agreement with divertor *H*-mode discharges, the D_α signals for all chords are in phase with each other. This is demonstrated in Fig. 3 where signals are plotted for D_α detectors viewing the edge plasma located at poloidal angles of 7° and 25° above the midplane.

In TFTR, the D_α bursts appear to be preceded by high-frequency magnetic oscillations¹⁴ [see \tilde{B}_θ signal plotted in Fig. 3(d)]. The mode number of these magnetic oscillations is found to be $m/n = 1/0$ in the frequency range 50–500 kHz. This is the first observation of a high-frequency oscillation during ELMs, with an

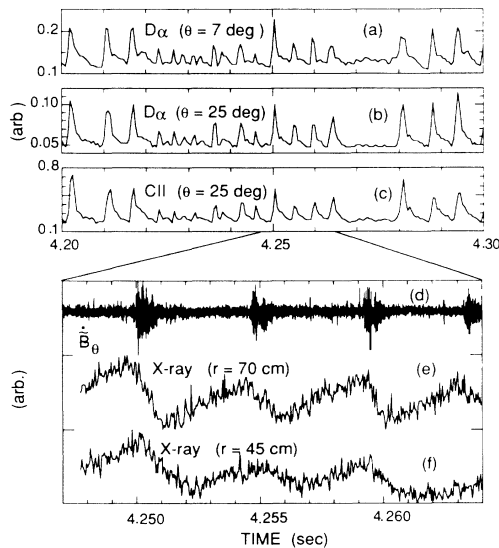


FIG. 3. Time correlation of D_α signals for the plasma edge at poloidal angles of 7° and 25° above the midplane of an 80-cm minor-radius discharge. Mirnov loop (\tilde{B}_θ), soft-x-ray, and C II signals are also plotted. $R = 2.45 \text{ m}$, $B_\phi = 4 \text{ T}$, $I_p = 0.9 \text{ MA}$, $P_b = 13 \text{ MW}$. Shot No. 44008.

$n=0$ component. Measurements of electron cyclotron emission (ECE) during ELMs, using a grating polychromator, sometimes show 20–30- μs -duration intense emission spikes which occur simultaneously with the beginning of the magnetic oscillations. The spikes are consistent with dumping of electrons, from a volume 15–20 cm within the plasma edge. These electrons move radially outward at a velocity $\approx (2-3) \times 10^5 \text{ cm/s}$.¹⁵ The soft-x-ray signal for the viewing chord with tangency radius of $r = 70 \text{ cm}$ ($a_p = 80 \text{ cm}$) begins to drop approximately at the beginning of the magnetic oscillations. The soft-x-ray signal for the chord at $r = 45 \text{ cm}$ drops $\approx 0.6 \text{ ms}$ after that for the chord at $r = 70 \text{ cm}$, indicating that the ELM disturbance is initiated at the plasma edge, and that the resulting edge cooling and subsequent reheat propagate radially inward.

Recently, there has been interest in poloidal rotation and radial electric fields associated with the *H* mode.^{16,17} On DIII-D,¹⁶ a poloidal “spin up” in the $-\mathbf{E}_r \times \mathbf{B}_\phi$ direction has been observed during the *L*- to *H*-mode transition. Evidence of similar behavior on TFTR is provided by microwave scattering measurements of density fluctuations.¹⁵ The measurements show an edge feature during the *H* mode for $f > 0.8 \text{ MHz}$ (at $k_\perp \approx 5 \text{ cm}^{-1}$) in the scattered spectrum, which is consistent with a wave at the plasma edge propagating in the electron diamagnetic drift direction. On TFTR, this would be in the direction of a poloidal velocity ($v_\theta \approx 10^4 \text{ m/s}$) arising from an inwardly directed E_r . Attempts are being made

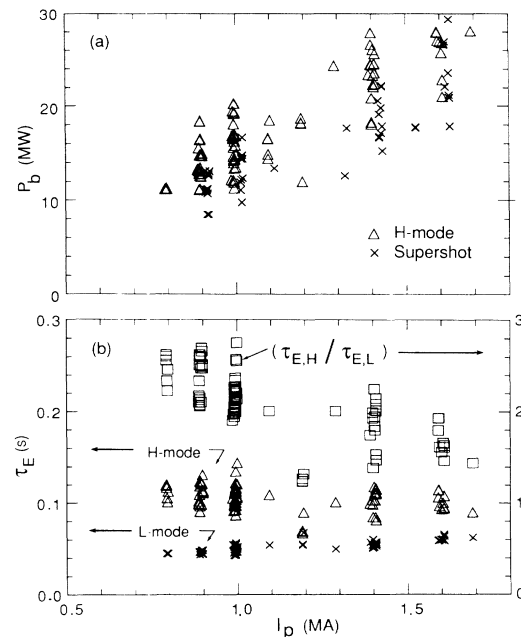


FIG. 4. (a) Plot of P_b vs I_p for the TFTR limiter *H* mode. Data for supershots are also included (but only a small fraction of the TFTR supershot database). An apparent threshold power dependence on I_p is indicated. (b) τ_E from magnetics for the *H* mode, for *L*-mode scaling, and their ratio as a function of I_p . $B_\phi = 3.0$ to 5.2 T .

to measure v_θ (using the CHERS system in a way similar to DIII-D) on TFTR to compare with theoretical models for the H mode.

The discharge of Fig. 1 is one of a number of limiter H modes obtained using an I_p of 0.8 MA and balanced beam power, $P_b = 11$ MW. These are the lowest values of I_p and P_b at which limiter H modes have been obtained on TFTR. In general, the threshold power required to trigger a transition appears to have an I_p dependence. This is apparent in Fig. 4, which includes plots of P_b and τ_E vs I_p for the full range of TFTR H -mode plasmas. For I_p in the range 0.8 to 1.0 MA, the minimum P_b required for a transition to occur is ≈ 11 MW, while at 1.4 MA, 18 MW are required, and at 1.6 MA a slightly higher value of ≈ 21 MW of NBI is needed. On a given day the boundary in P_b - I_p space can be relatively sharp. For example, at $P_b \approx 14$ MW a shot-to-shot change in I_p as small as 50 kA, from 1.0 to 1.05 MA, was sufficient to block the transition to the H mode. On the other hand, the threshold power for a given I_p deduced from Fig. 4(a) is not precise since the data were collected over many weeks of operation. Uncertainties are introduced due to day-to-day variation in limiter conditioning, cobeam-counterbeam mixture, and sawtooth activity.¹⁸

The values of τ_E plotted in Fig. 4(b) are only for low-recycling conditions. Limiter H modes with enhanced confinement have been realized on TFTR only under low-recycling conditions where the transition is from the supershot to the H regime. The ratio of τ_E of the H mode to $\tau_{E,L\text{-mode}}$ [Fig. 4(b)] can be > 2.5 . However, although there is an increase in n_e at the edge, the improvement in particle confinement appears to be less than observed on divertor tokamaks. This conclusion is supported by x-ray pulse-height-analyzer measurements which show the metal concentration to remain fairly constant (no accumulation) during the H -mode phase.

In summary, a peaked-density H -mode discharge with $\tau_E > 2.5$ times L -mode scaling has been obtained in a circular TFTR limiter configuration. The density peaking factor can be > 2.3 , and the transition is usually from a supershot to the H mode. Most of the standard features associated with the H mode are observed. For many of the H modes studied so far, the ELMs were found to be preceded by or coincident with a high-frequency magnetic oscillation. These peaked-density-profile H modes may offer an alternative scenario for future tokamaks such as the CIT and ITER.

We wish to thank K. M. Young for his suggestions and continued support. We also express our appreciation

for the dedication and support of the TFTR physicists and staff. This work was supported by the U.S. Department of Energy Contract No. DE-AC02-76-CH0-3073.

^(a)On assignment from Oak Ridge National Laboratory, Oak Ridge, TN 37831.

^(b)On assignment from Los Alamos National Laboratory, Los Alamos, NM 87545.

¹K. Odajima *et al.*, in *Proceedings of the Eleventh IAEA Conference on Plasma Physics and Controlled Nuclear Fusion Research, Kyoto, 1986*, edited by J. W. Weil and M. Demir (International Atomic Energy Agency, Vienna, 1987), Vol. 1, p. 151.

²S. Sengoku *et al.*, *Phys. Rev. Lett.* **59**, 450 (1987).

³H. Matsumoto *et al.*, in *Proceedings of the Fourteenth European Conference on Controlled Fusion and Plasma Physics, Madrid, Spain, 1987*, edited by F. Engelmann and J. L. Alvarez Rivas (European Physical Society, Petit-Lancy, Switzerland, 1987), Vol. 11D, Pt. I, p. 5.

⁴K. Toi *et al.*, in *Proceedings of the Sixteenth European Conference on Controlled Fusion and Plasma Physics, Venice, Italy, 1989* (European Physical Society, Petit-Lancy, Switzerland, 1989), Vol. 13B, Pt. I, p. 221.

⁵D. P. Schissel *et al.*, in *Proceedings of the Sixteenth European Conference on Controlled Fusion and Plasma Physics, Venice, Italy, 1989* (Ref. 4), p. 115.

⁶J. D. Strachan *et al.*, *Phys. Rev. Lett.* **58**, 1004 (1987).

⁷R. J. Goldston, *Plasma Phys. Controlled Fusion* **26**, 87 (1984).

⁸F. Wagner *et al.*, *Phys. Rev. Lett.* **49**, 1408 (1982).

⁹S. M. Kaye *et al.*, *J. Nucl. Mater.* **121**, 115 (1984).

¹⁰H. F. Dylla *et al.*, *Nucl. Fusion* **27**, 1221 (1987).

¹¹B. J. D. Tubbing *et al.*, *Nucl. Fusion* **29**, 1953 (1989).

¹²K. McGuire *et al.*, *Phys. Fluids B* **2**, 1287 (1990); K. McGuire *et al.*, in *Proceedings of the Ninth International Conference on Plasma Surface Interactions in Controlled Fusion Devices, Bournemouth, United Kingdom, 21-25 May 1990* [*J. Nucl. Mater.* (to be published)].

¹³R. V. Budny *et al.*, *J. Nucl. Mater.* **162-164**, 214 (1989).

¹⁴S. M. Kaye *et al.*, Princeton Plasma Physics Laboratory Report No. PPPL-2687, 1990 (to be published); R. Bell *et al.*, *Phys. Fluids B* **2**, 1271 (1990).

¹⁵C. E. Bush *et al.*, in *Proceedings of the Eighth Topical Conference on High-Temperature Plasma Diagnostics, Hyannis, Massachusetts, 6-10 May 1990* [*Rev. Sci. Instrum.* (to be published)].

¹⁶R. J. Groebner *et al.*, in *Proceedings of the Sixteenth European Conference on Controlled Fusion and Plasma Physics, Venice, Italy, 1989* (Ref. 4), p. 245.

¹⁷R. J. Taylor *et al.*, *Phys. Rev. Lett.* **63**, 2365 (1989).

¹⁸F. Wagner *et al.*, *J. Nucl. Mater.* **121**, 103 (1984).